Synthesis and Catalytic Evaluation of Dendrimer-Encapsulated Cu Nanoparticles

An Undergraduate Experiment Exploring Catalytic Nanomaterials

Z. Vivian Feng,*† Jennifer L. Lyon, J. Sawyer Croley, Richard M. Crooks, David A. Vanden Bout, and Keith J. Stevenson

Freshman Research Initiative, Department of Chemistry and Biochemistry, University of Texas at Austin, Austin, TX 78712;
**feng@augsburg.edu*

Although some effort has been made to introduce new educational concepts related to the study of nanomaterials to undergraduates, very few laboratory methods and instructional materials have been created concerning the synthesis and characterization of nanomaterials in the undergraduate chemistry curriculum on a large scale *(1–6)*. A newly funded NSF program at this university, which we call the Freshman Research Initiative, has enabled us to develop an undergraduate chemistry curriculum that exposes undergraduates, primarily first-year students, to authentic research in various fields, including nanoscience. Herein, we report the development of a new multi-component laboratory module that focuses on (i) the synthesis of copper nanoparticles prepared using dendrimers as a structure-directing template to control the particle size and stability, (ii) the characterization of the chemical and structural properties of the nanoparticles using UV–vis spectroscopy, and (iii) performance evaluation of the nanoparticles as catalysts for the reduction of *p*-nitrophenol using UV–vis spectroscopy.

In recent years, the synthesis of nanoscopic materials, materials containing nanoparticles ranging in size of 1–100 nm, has attracted a great deal of interest because such materials typically exhibit properties that differ from bulk materials of the same composition. In no field of study is this more apparent than in the area of catalysis, as catalytic performance is markedly enhanced as a result of the increased surface area of nanomaterials relative to their bulk counterparts. Catalysts are important to many technological processes including energy production, energy conversion, environmental remediation, pollution abatement, and specialty chemical production *(7–9)*. A key area of research is the development of new synthetic methods that will allow for the rational design of efficient catalysts of controlled size and composition. Equally important is a fundamental understanding of the structure–activity relationships that govern catalysts in chemical reactions.

In part I of this laboratory module, we describe how macromolecular polymers known as dendrimers can be used to prepare dendrimer-encapsulated metal nanoparticles (metal–DEN). An array of monometallic and bimetallic nanoparticles has been successfully synthesized with this method, such as Pt *(10, 11)*, Pd *(11, 12)*, Au *(13, 14)*, Pd–Au *(15)*, Pt–Cu *(16)*, Au–Ag *(17)*, and Pt–Pd *(9, 18)*. In this case, Cu–DEN is prepared using a synthetic method that incorporates a fourth-generation (G4) poly(amidoamine) (PAMAM) dendrimer. With an appropriate ratio of dendrimer to copper ion and solution pH, copper ions partition into the dendrimer interior, where they complex with interior tertiary amine groups. Reduction of the dendrimer–copper-ion composites with a chemical reducing agent (e.g., $NaBH_4$) added in stoichiometric excess produces zero-valent, dendrimer-encapsulated Cu nanoparticles. The preparation of Cu nanoparticles using a dendrimer template is advantageous in that this synthesis yields nanosized Cu particles that are stabilized by dendrimer encapsulation to prevent agglomeration or precipitation, while providing accessible catalytic surfaces.

Part II of this laboratory module describes how UV–vis spectroscopy can be used to evaluate the catalytic performance of Cu–DEN using a model reaction involving the reduction of *p*-nitrophenol to *p*-aminophenol. We chose this model reaction because nitrophenols are among the most prevalent organic pollutants in wastewaters generated from agricultural and industrial sources, including companies that manufacture explosives, dyestuffs, and other products *(19–21)*. Nitrophenols are considered hazardous wastes and priority toxic pollutants by the U.S. Environmental Protection Agency. Therefore, it is important to assess the fate of these compounds in the environment and develop effective methods to remove them from water.

From an educational standpoint, this laboratory emphasizes concepts of pH, metal ion complexation, Brønsted–Lowry and Lewis acid–base chemistry, catalysts, kinetics, and redox reactions, all of which are covered in most general chemistry curricula but are often difficult for undergraduates to grasp. Through a hands-on, experimental laboratory approach, students can gain a deeper understanding of these concepts and develop a greater appreciation of laboratory methods in the study of nanomaterials. Students are also exposed to an actively developing research field and current research literature in the areas of nanoparticle synthesis, spectroscopic characterization, and catalytic evaluation *(17, 22–24)*. The experiments are flexible enough so that this laboratory module can be implemented either as a sequence of structured introductory general chemistry experiments or as a more open-ended, upper-division analytical, physical, or materials chemistry project.

Experimental

Materials and Equipment

The chemicals needed for this project are readily available from commercial sources. Fourth generation PAMAM dendrimer with hydroxyl terminal (G4-OH) in methanol (10% w/w, Aldrich), $CuSO_4{\cdot}5H_2O$ (Fisher), hydrochloric acid (Fisher), sodium hydroxide (Fisher), and sodium borohydride (Aldrich) were used as received. The water used in the laboratory was purified by a Barnstead Nanopure system (≥ 18.2 MΩ cm). Syringe filters with 0.20 μm pore size (Corning) were used to filter the Cu–DEN solutions before use in the catalysis studies.

Spectrophotometric titrations and absorption spectra were obtained using a 10 mm path length cuvette with an Agi-

---

[†] Current address: Department of Chemistry, Augsburg College, Minneapolis, MN, 55454.

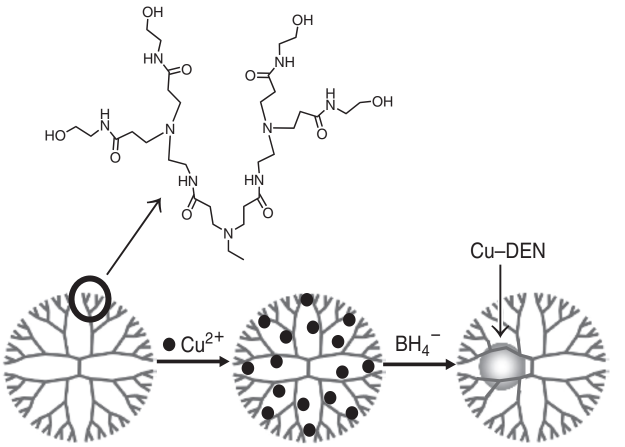

Scheme I. Dendrimer template-assisted synthesis of Cu nanoparticles.

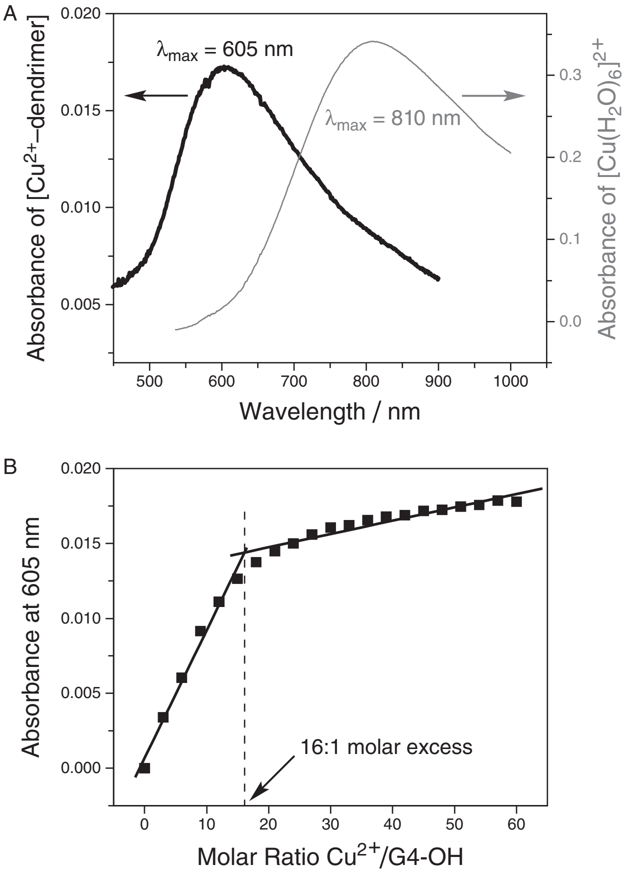

Figure 1. Absorption spectra of (A) Cu^{2+}-loaded G4-OH dendrimer solution (thick line, left scale), and Cu^{2+} in water without dendrimer ([Cu(H$_2$O)$_6$]$^{2+}$ complex; thin line, right scale), and (B) spectrophotometric titration of Cu^{2+} with G4-OH dendrimers monitored at 605 nm at pH 5.7. Note that the scales are different in (A) reflective of the change in molar absorptivites for Cu–ligand complexes.

lent 8453 UV–vis spectrophotometer equipped with kinetics module software so that time dependent absorption spectra can be obtained at multiple wavelengths. pH measurements were made with a Vernier LabPro system, pH sensor, and LoggerPro software.

Hazards

Sodium borohydride is a strong reducing agent, is corrosive, and may cause burns to any area of contact. It is also a flammable solid. Sodium hydroxide and hydrochloric acid are corrosive. *p*-Nitrophenol is poisonous via inhalation, swallowing, and contact with the skin. Copper(II) sulfate can cause irritation to skin, eyes, and respiratory tract.

Results and Discussion

Part I: Synthetic Procedure

The synthesis protocol for Cu–DEN is adapted from a previously established procedure *(23, 25)* where Cu nanoparticles are synthesized by complexing copper ions to the interior amine groups of G4-OH dendrimers followed by chemical reduction of the complexed copper cations using sodium borohydride ($NaBH_4$) to form encapsulated zero-valent Cu particles as shown in Scheme I. An experimental flow chart and solution preparation guidelines are provided as online materials. In the absence of dendrimer, the blue solution color and absorption spectrum of a $CuSO_4$ solution corresponds to the presence of $[Cu(H_2O)_6]^{2+}$, which exhibits a broad, weak absorbance band centered at 810 nm (Figure 1A). The absorption spectrum associated with the complexation of Cu^{2+} within the dendrimer, a broad absorbance band centered at 605 nm, is also shown in Figure 1A. The Cu^{2+} complexation process can be followed by spectrophotometric titration at 605 nm where intensity increases as more Cu^{2+} is added to the G4-OH dendrimer solution (Figure 1B). The absorbance at 605 nm levels off after roughly 16 molar excess equivalents of Cu^{2+} are added, signifying the titration endpoint and that 16 molar equivalents of Cu^{2+} have coordinated with the maximum number of interior amines sites. Since a G4-OH dendrimer contains 62 interior amine groups, the spectrophotometric titration suggests that one Cu^{2+} is coordinated to a maximum of four amine groups; however, a more thorough analysis of binding interactions and the consideration of dendrimer structure indicates that on average one Cu^{2+} is associated with two amine groups *(25)*. At 16 molar equivalent, the Cu clusters formed are most likely less than 1 nm in diameter. Unfortunately, since Cu is a low *Z* element, simple size characterization by means of transmission electron microscopy (TEM) is difficult, even for Cu particles synthesized at higher molar equivalents *(25)*.

A representative absorbance spectrum for the Cu–DEN solution after reduction is shown in Figure 2 and can be compared to the unreduced Cu^{2+}-loaded G4-OH dendrimer solution in Figure 1A. In comparison to the unreduced spectrum, the reduced Cu–DEN solution (Figure 2) displays an elevated baseline at lower visible wavelengths along with the disappearance of the Cu^{2+} absorbance at 605 nm, indicating the formation of Cu–DEN. Lack of any plasmon peak at 570 nm suggests that the Cu nanoparticles have diameters less than 5 nm *(25)*. Students should be encouraged to acquire their own UV–vis spectra and compare characteristic features with both visual and reported literature observations *(23, 25)*.

The Cu–DEN synthesis process requires pH control (see the online material). Most of the students indicated that out of the entire laboratory procedure, they were most challenged

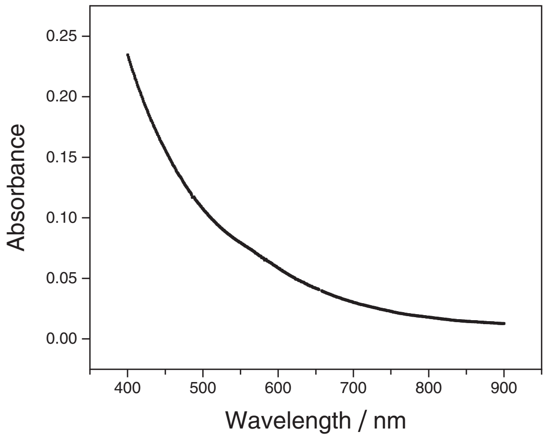

Figure 2. Absorption spectrum of Cu^{2+}-loaded G4-OH dendrimer solution after reduction (Cu–DEN).

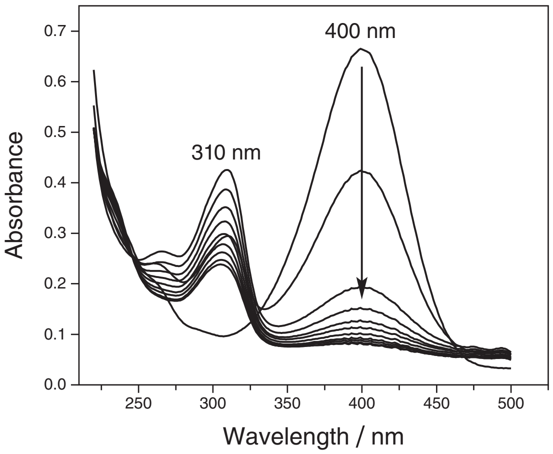

Figure 3. Time-based UV–vis spectra monitoring *p*-nitrophenol reduction catalyzed by Cu–DEN. The spectra were recorded every 5 s for 240 s. Only time points corresponding to 10 s intervals for the first 100 s are shown for better clarity. The reaction mixture contains 600 µL filtered Cu–DEN solution, 250 µL of 600 µM *p*-nitrophenol, 1.50 mL of 0.10 M $NaBH_4$, and 1.60 mL H_2O.

by the pH adjustment during synthesis of Cu–DEN. Many students have reproduced a pH titration curve in the laboratory similar to those shown in their general chemistry textbooks, yet most have not considered the consequences of pH control in a real experimental scenario. In the laboratory, students were also often frustrated by the drastic pH change (overshoot) that occurred when a small quantity of a strong acid (e.g., 0.1 M HCl) or a strong base (e.g., 0.1 M NaOH) was added to unbuffered dendrimer solutions of near-neutral pH. This experimental result provided a great opportunity to remind them that the pH scale is not linearly proportional to the quantity of protons, H^+, but is based on a logarithmic scale. From these experimental exercises, students were genuinely impressed by the complexity of acid–base and metal ion coordination chemistry. Synthesis of Cu–DEN in buffered solution is planned to be investigated in future experiments.

Part II: Catalytic Evaluation Procedure

In basic aqueous solution (pH ≥ 10), *p*-nitrophenol exhibits a bright yellow color with an absorbance peak at 400 nm. The addition of Cu–DEN with $NaBH_4$ catalyzes the reduction of *p*-nitrophenol

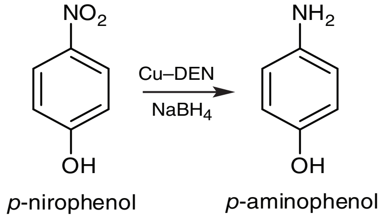

resulting in both a decrease in the absorbance peak centered at 400 nm and the appearance of an absorbance band at 310 nm corresponding to the formation of *p*-aminophenol *(24)*. This reaction can be catalyzed with Cu–DEN and several other types of noble metal nanoparticles *(26, 27)* and is a pseudo-first-order reaction when $NaBH_4$ is added in large excess to the Cu–DEN catalyst and *p*-nitrophenol *(17)*. We note that the mechanism of this reaction involves a more complicated set of reaction intermediates than outlined and still remains a point of considerable debate *(27)*. However, has been generally accepted that the absorbance band at 310 nm signifies the formation of a stable reduction product, *p*-aminophenol. Therefore, the natural logarithm of the absorbance at 400 nm, $A_{400}(t)$, corresponding to the disappearance of *p*-nitrophenol at any given time, is expected to be linear with time

$$\ln A_{400}(t) \;=\; -kt \;+\; \ln A_{400}(0) \qquad (1)$$

where k is the rate constant and $A_{400}(0)$ is the initial absorbance at 400 nm. By plotting the natural logarithm of the absorbance values at 400 nm over time, the rate constant, k, can be determined by the slope.

An example of time-based spectra of the *p*-nitrophenol reduction reaction monitored in the UV–vis region over a period of 240 s (4 min) with 5 s time intervals is shown in Figure 3 (only spectra of every 10 s for the first 100 s are shown for clarity). At the beginning of the reaction, the prominent feature at 400 nm is the signature of deprotonated *p*-nitrophenol (*p*-nitrophenolate) in basic media, which corresponds to the yellow color of the *p*-nitrophenolate solution. Upon the addition of $NaBH_4$, the peak at 400 nm decreases over the time period of the experiment. The peak at 310 nm indicates the formation of *p*-aminophenol. The absorbance values at 400 nm can then be exported to a spreadsheet and plotted as a function of time, shown in Figure 4A. Since freshly prepared $NaBH_4$ bubbles vigorously, an entire spectrum may shift if a gas bubble appears in the light path of the spectrophotometer and thus reduces the path length, resulting in a lower observed absorbance. Therefore, the absorbance at 600 nm, where the spectrum is featureless, is also recorded at each time interval and is subtracted from the absorbance at 400 nm to correct for such possible drifts. Furthermore, it is also important to plot the natural log of the “corrected absorbance”, obtained by plotting the natural log of the absorbance at time t, $A_{400}(t)$, minus the absorbance at time final, $A_{400}(t_{\mathrm{final}})$, as seen in Figure 4B. Plotting the data in this fashion facilitates more precise estimation of the linear region

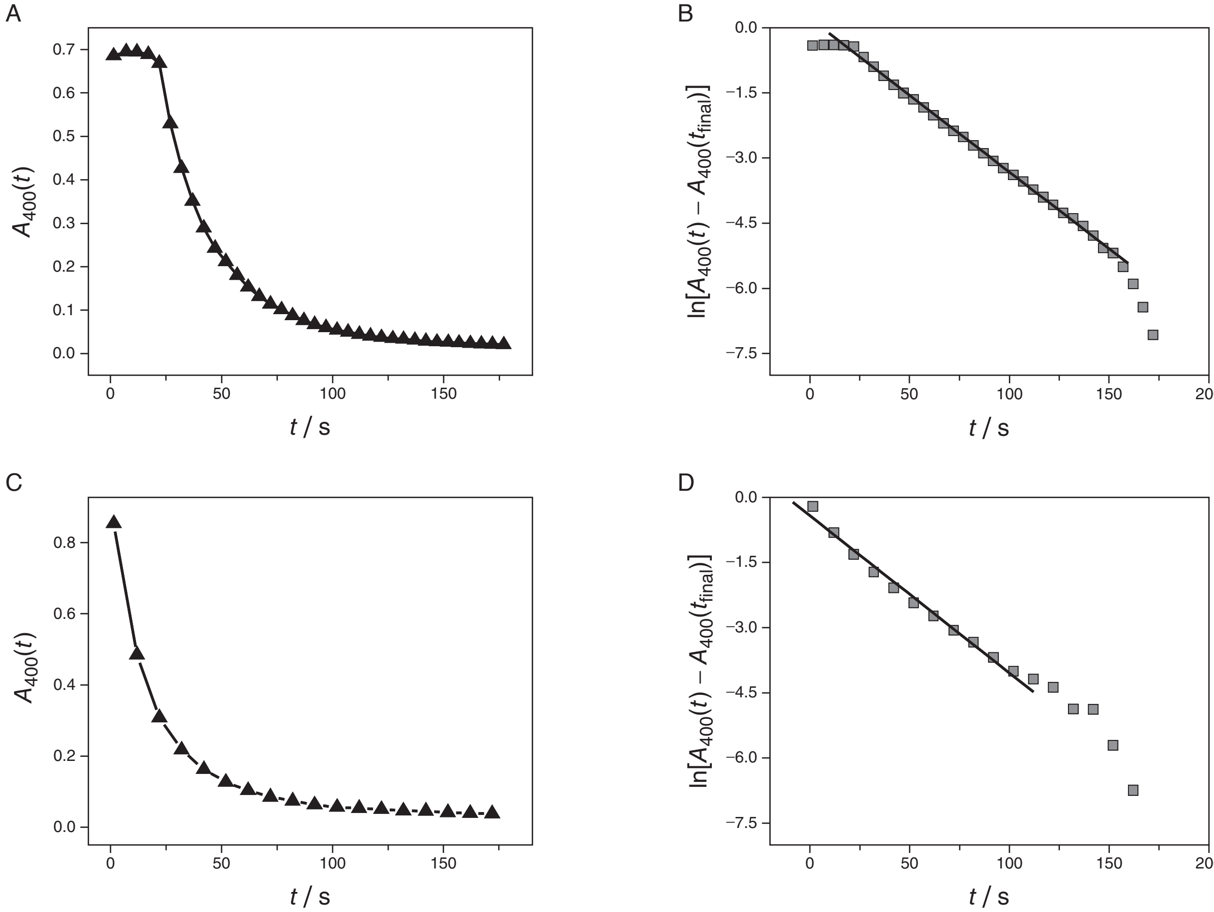

Figure 4. Absorbance at 400 nm plotted over time for reactions in which (A and B) $NaBH_4$ is added last and (C and D) *p*-nitrophenol is added last. (B) and (D) First-order kinetic plots for the absorbance at 400 nm of the curves shown in (A) and (C), respectively.

associated with measurement of the rate constant, *k*. The data in Figure 4A clearly indicate the onset of *p*-nitrophenol reduction as evidenced by the time dependent decrease in absorbance at 400 nm. Within 3 minutes, *p*-nitrophenol was almost completely consumed, as illustrated by the flattened tail end of the plot and a resulting colorless solution.

We note that in the colorimetric monitoring of *p*-nitrophenol reduction, an unexpected induction period can be seen, shown as the initial horizontal portion of the curve ($t < 25$ s) in Figure 4A. The length of this period depends on the age of the Cu–DEN solution. Since Cu^0 is readily oxidized to copper oxides if exposed to air for extended periods of time, an induction period can occur as time is required for $NaBH_4$ to re-reduce surface oxides on the Cu–DEN, reactivating the Cu–DEN to catalyze the reduction of *p*-nitrophenol. We emphasize that students should be encouraged to conduct experiments in which the same reaction components are used, but are added in different order. An example of the resulting absorbance versus time plot is shown in Figure 4C, where $NaBH_4$ is added first and *p*-nitrophenol is added last to initiate the reaction. Clearly, the induction period is reduced from over 25 s to 0 s, while other features such as slope remain unchanged.

The corresponding first-order kinetic plots for *p*-nitrophenol reduction are shown in Figures 4B and 4D. Both Figures 4B and 4D clearly demonstrate linear behavior after the induction period with slopes of -0.035 s^{-1} and -0.037 s^{-1} when *p*-nitrophenol is added first and then last, respectively. We note that these results demonstrate that adding either *p*-nitrophenol or $NaBH_4$ last affects only the duration of the induction period, not the rate constant. However, the apparent rate constant can vary depending on student skill and mastery of lab technique. For instance, experiments conducted by a class of 14 students yielded rate constants varying from 0.028 to 0.040 s^{-1}.

To further illustrate the importance of using a Cu–DEN catalyst, students should be encouraged to perform control experiments by carrying out uncatalyzed *p*-nitrophenol reductions (i.e., without the presence of Cu–DEN, but in the presence of G4-OH dendrimers). Importantly, the students will find that over the course of ~30 minutes, the absorbance peak at 400 nm for *p*-nitrophenol barely decreases (data not shown). Data analysis for uncatalyzed *p*-nitrophenol reduction yields a rate constant of $\sim 4.0 \times 10^{-4}$ s^{-1}, which is nearly two orders of magnitude smaller than the reaction catalyzed by Cu–DEN. If time permits, students should be also encouraged to vary one or more of the experimental parameters (e.g., changing the ratio or concentration of solution components) to observe the influence on the apparent rate constant.

Kinetics, especially integrated rate laws, is often a difficult concept for first-year chemistry students to grasp because there are limited laboratory experiments that serve as good visual aids to increase understanding. We found this experiment to be an excellent exercise for the purpose of illustrating first-order rate laws, role of catalyst, and other kinetic concepts. Both catalyzed and uncatalyzed reactions can be performed within a reasonable time, with a simple experimental setup, to help students understand the importance of a catalyst for facilitating chemical reactions. A few of our more advanced students who finished the experiment early proposed and tested the effect of catalyst concentration on the rate of the reaction. With rather simple data analysis, students had first-hand experience in extrapolation of a rate constant from a first-order integrated rate law plot. If a temperature-controlled environment can be established in the spectrophotometer cell holder, the Arrhenius relationship can be explored, and the activation energy determined to better explain the concept of catalysis.

Conclusion

The experiments described in this two-part module incorporate several fundamental concepts introduced into the undergraduate chemistry curriculum in the unique context of nanomaterials evaluated as catalysts. Students can successfully synthesize and characterize dendrimer-encapsulated Cu nanoparticles, and evaluate these materials as catalysts for the reduction of *p*-nitrophenol using UV–vis spectroscopy (colorimetry). We found that student understanding of Bronsted–Lowry and Lewis acid–base chemistry, pH, Beer–Lambert law and kinetics increased dramatically. By bringing active research literature into the teaching laboratory, we have also successfully broken down the students' mental barrier in understanding current peer-reviewed literature. When given ample time to replicate their results and to complete the project (3 weeks), the students demonstrated significant interest and motivation and were eager to improve the experimental design and to test more experimental parameters.

Acknowledgments

This work was supported by the National Science Foundation (Award No. 0629136), and the Freshman Research Initiative (FRI) program, College of Natural Sciences at the University of Texas at Austin. We thank our FRI "Nano stream" students Spring class of 2007 for pioneering this laboratory module. R.M.C. acknowledges the support by the National Science Foundation (Grant No. CHE-0531030).

Literature Cited

1. Bentley, A. K.; Farhoud, M.; Ellis, A. B.; Lisensky, G. C.; Nickel, A. M. L.; Crone, W. C. *J. Chem. Educ.* **2005,** *82,* 765.
2. Dungey, K. E.; Muller, D. P.; Gunter, T. *J. Chem. Educ.* **2005,** *82,* 769.
3. Solomon, S. D.; Bahadory, M.; Jeyarajasingam, A. V.; Rutkowsky, S. A.; Boritz, C.; Mulfinger, L. *J. Chem. Educ.* **2007,** *84,* 322.
4. Keating, C. D.; Musick, M. D.; Keefe, M. H.; Natan, M. J. *J. Chem. Educ.* **1999,** *76,* 949.
5. Williams, G. L.; Vohs, J. K.; Brege, J. J.; Fahlman, B. D. *J. Chem. Educ.* **2005,** *82,* 771.
6. Winkelmann, K.; Noviello, T.; Brooks, S. *J. Chem. Educ.* **2007,** *84,* 709.
7. Vijayaraghavan, G.; Stevenson, K. J. *Langmuir* **2007,** *23,* 5279.
8. Garcia-Martinez, J. C.; Lezutekong, R.; Crooks, R. M. *J. Am. Chem. Soc.* **2005,** *127,* 5097.
9. Scott, R. W. J.; Datye, A. K.; Crooks, R. M. *J. Am. Chem. Soc.* **2003,** *125,* 3708.
10. Xie, H.; Gu, Y. L.; Ploehn, H. J. *Nanotechnology* **2005,** *16,* S492.
11. Ye, H. C.; Scott, R. W. J.; Crooks, R. M. *Langmuir* **2004,** *20,* 2915.
12. Scott, R. W. J.; Ye, H. C.; Henriquez, R. R.; Crooks, R. M. *Chem. Mater.* **2003,** *15,* 3873.
13. Hayakawa, K.; Yoshimura, T.; Esumi, K. *Langmuir* **2003,** *19,* 5517.
14. Kim, Y. G.; Oh, S. K.; Crooks, R. M. *Chem. Mater.* **2004,** *16,* 167.
15. Scott, R. W. J.; Wilson, O. M.; Oh, S. K.; Kenik, E. A.; Crooks, R. M. *J. Am. Chem. Soc.* **2004,** *126,* 15583.
16. Hoover, N. N.; Auten, B. J.; Chandler, B. D. *J. Phys. Chem. B* **2006,** *110,* 8606.
17. Endo, T.; Yoshimura, T.; Esumi, K. *J. Colloid Interf. Sci.* **2005,** *286,* 602.
18. Chung, Y. M.; Rhee, H. K. *Catal. Lett.* **2003,** *85,* 159.
19. Iinuma, Y.; Bruggemann, E.; Gnauk, T.; Muller, K.; Andreae, M. O.; Helas, G.; Parmar, R.; Herrmann, H. *J. Geophys. Res.* **2007,** *112,* D08209. Doi:10.1029/2006JD007120.
20. Mori, T.; Watanuki, T.; Kashiwagura, T. *Environ. Toxicol.* **2007,** *22,* 58.
21. Li, C. M.; Taneda, S.; Suzuki, A. K.; Furuta, C.; Watanabe, G.; Taya, K. *Toxicol. Appl. Pharmacol.* **2006,** *217,* 1.
22. Scott, R. W. J.; Wilson, O. M.; Crooks, R. M. *J. Phys. Chem. B* **2005,** *109,* 692.
23. Zhao, M. Q.; Sun, L.; Crooks, R. M. *J. Am. Chem. Soc.* **1998,** *120,* 4877.
24. Endo, T.; Kuno, T.; Yoshimura, T.; Esumi, K. *J. Nanosci. Nanotechnol.* **2005,** *5,* 1875.
25. Zhao, M. Q.; Crooks, R. M. *Chem. Mater.* **1999,** *11,* 3379.
26. Pradhan, N.; Pal, A.; Pal, T. *Langmuir* **2001,** *17,* 1800.
27. Corma, A.; Conception, P.; Serna, P. *Angew. Chem., Int. Ed.* **2007,** *46,* 7266.

Supporting *JCE Online* Material

http://www.jce.divched.org/Journal/Issues/2009/Mar/abs368.html

Abstract and keywords

Full text (PDF)
    Links to cited *JCE* articles

Supplement
    Student handouts including an experimental flow chart
    Instructor notes including a preparation guide for the solutions